nature geoscience

Article

https://doi.org/10.1038/s41561-024-01577-0

Low-elevation forest extent in the western United States constrained by soil surface temperatures

Received: 17 December 2023

Accepted: 29 September 2024

Published online: 19 November 2024

Check for updates

Zachary A. Holden[1] ✉, Solomon Z. Dobrowski[2], Alan Swanson[3], Zachary Hoylman[2,4], Drew Lyons[5], Allen Warren[3] & Marco Maneta[6]

Climate change and disturbance threaten forested ecosystems across the globe. Our ability to predict the future distribution of forests requires understanding the limiting factors for regeneration. Forest canopies buffer against near-surface air temperature and vapour pressure deficit extremes, and ongoing losses of forest canopy from disturbances such as wildfire can exacerbate climate constraints on natural regeneration. Here we combine experimental, empirical and simulation-based evidence to show that soil surface temperatures constrain the low-elevation extent of forests in the western United States. Simulated potential soil surface temperatures predict the position of the low-elevation forest treeline, exhibiting temperature thresholds consistent with field and laboratory studies. High-resolution historical and future surface temperature maps show that 107,000–238,000 km^2 (13–20%) of currently forested area exceeds the critical thermal threshold for forest regeneration and this area is projected to more than double by 2050. Soil surface temperature is an important physical control on seedling survival at low elevations that will likely be an increasing constraint on the extent of western United States forests as the climate warms.

Forests are the dominant terrestrial ecosystem on the planet. They are critical stores of carbon, reservoirs of biodiversity and provide invaluable ecosystem services for society[1–3]. Risks to forests are now more widespread than in the recent past owing, in part, to changes in the Earth's climate, which is becoming increasingly inhospitable to sustaining forests in some regions[3,4]. Changes in forest area can have profound consequences for the hydrology, biogeochemistry, ecology and regional economies of forested regions globally[5]. The importance of disturbance and post-disturbance recovery dynamics has become increasingly clear as increases in the frequency of heat and drought events have been linked to increased area burned[6], forest mortality[4,7] and recruitment limitations[8,9], all of which increase the likelihood of ecosystem transitions if trees are unable to regenerate at sites they previously occupied[10].

Semi-arid forests near low-elevation treelines are particularly vulnerable to climatic effects because they occupy marginal conditions for tree recruitment owing to drought and heat stress. In contrast to upper treelines, which have been the focus of decades of research[11,12], the climatic drivers of low-elevation treeline are less well understood. Nonetheless, the importance of this ecosystem boundary is clear; relative to upper treeline, small deviations in the lower treeline position result in large changes in forested area owing to greater land area at

[1]USDA Forest Service Rocky Mountain Research Station, Missoula, MT, USA. [2]Franke College of Forestry and Conservation, University of Montana, Missoula, MT, USA. [3]Department of Community and Public Health Sciences, University of Montana, Missoula, MT, USA. [4]Montana Climate Office, Franke College of Forestry and Conservation, University of Montana, Missoula, MT, USA. [5]Washington Department of Natural Resources, Olympia, WA, USA. [6]Geosciences Department, University of Montana, Missoula, MT, USA. ✉e-mail: zachary.holden@usda.gov

https://doi.org/10.1038/s41561-024-01577-0

low elevation[13]. Treeline dynamics are a function of multiple vital rates including growth and mortality responses in adult trees—processes that, in the short term, influence the current treeline position. In the long term, biophysical processes that influence the capacity of trees to regenerate better reflect the requirements for population persistence and expansion[14,15] and thus the extent of future forests.

Two principal biophysical mechanisms drive seedling mortality in semi-arid forests: loss of hydraulic function and lethal soil surface temperatures (SSTs)[16,17]. Relative to conspecific adults, seedlings are prone to succumb to drought and heat stress because of limited access to soil water, which reduces carbon acquisition for growth, metabolism and defence. Alternating periods of cool and wet versus hot and dry conditions drive episodic recruitment pulses, resulting in expansion and contraction of forests at lower treeline[18,19]. This suggests that hydroclimatic variation and recruitment dynamics play a prominent role in the areal extent of forests. Additionally, forest cover interacting with soil moisture creates microclimates that buffer temperature extremes near the ground surface[20–22]. Disturbance-driven loss of canopy cover can result in large increases in SST and vapour pressure deficit[23], which can kill seedlings by both increasing evaporative demand (and therefore hydraulic stress) and by directly damaging tissue where young plants are in contact with hot soil surfaces[24]. For example, in recently disturbed forests, SSTs can readily exceed 55 °C (ref. 25). Exposure to such extreme temperatures for even short periods of time kills young seedlings through the development of temperature-induced lesions on the stem[17].

Understanding the proximal mechanisms of seedling mortality is important for assessing, monitoring and forecasting risks to forest ecosystems. However, the linkages among drought, heat stress and mortality are complex and depend on biophysical processes that vary at fine spatio-temporal scales. Experimental research at the plant level has identified water potential thresholds in the soil and within the plant below which hydraulic function is compromised[26,27]. These thresholds have been used to map forest mortality risk using empirically derived stress metrics[7,28] and, to a more limited extent, using mechanistic models that simulate plant hydraulics[29]. Similarly, a long history of experimental work with conifer seedlings has focused on the development of time–dose response functions, which identify temperature thresholds at the soil surface that lead to seedling mortality[30]. Despite an extensive body of experimental and plant physiological research linking lethal temperatures to plant mortality, there has been limited work mapping these risks to forests.

Here, we combine experimental, empirical and simulation-based evidence to show that SSTs constrain the low-elevation extent of forests in the western United States through their direct effects on conifer seedling mortality. We introduce the concept of 'potential' SST (PSST)—the maximum temperature the ground surface would experience in the absence of overstory vegetation—as a means of assessing forest vulnerability. We simulate and map PSST using an ecohydrological model for the western United States, where PSST is defined as the 95th percentile annual 1982–2018 maximum SST that a site would experience given 10% forest canopy cover. Using 30 m resolution PSST maps, we (1) quantify its relationship to both existing tree cover and post-fire conifer recruitment across the western United States, (2) collate existing experimental data to define the thermal sensitivity of Ponderosa pine (*Pinus ponderosa* (PIPO)) and Douglas fir (*Pseudotsuga menziesii* (PSME)) seedlings to lethal surface temperatures, (3) demonstrate that the response functions in these experiments show congruent threshold behaviour with sharp declines in seedling survivorship, post-fire recruitment and forest cover when PSST is between 50 °C and 60 °C and (4) quantify potential changes in PSST as an indicator of future forest vulnerability to climate change.

Seedling sensitivity to extreme SSTs

Seedling mortality experiments with PSME and PIPO show sharp declines in survivorship with increasing SSTs between 50 °C and 60 °C

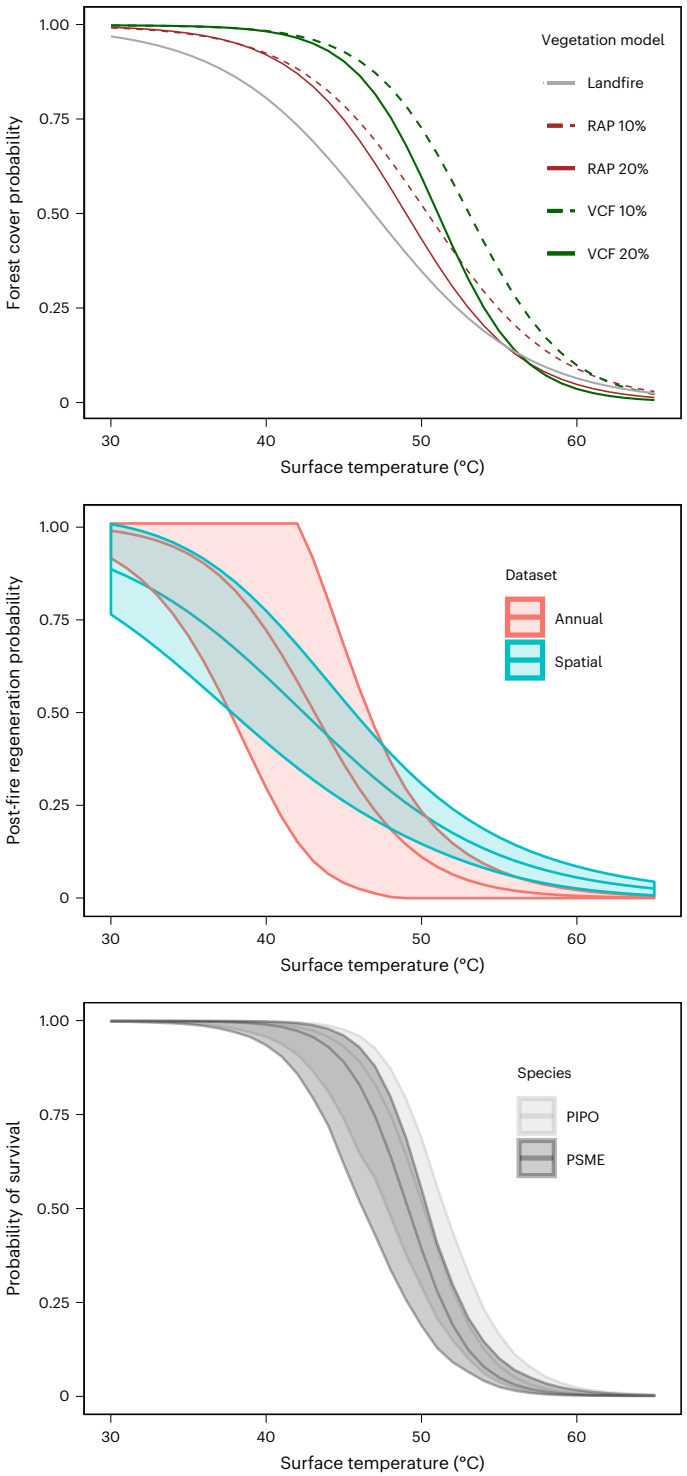

Fig. 1 | SST response functions. Results derived from logistic regression models from seedling experiments (bottom), post-fire regeneration data (middle) and remotely sensed forest cover (top), with s.d. for 95th percentile confidence intervals (shaded bands). Post-fire recruitment models include data representing space-for-time substitution (blue), where PSST represents the 1982–2018 95th percentile maximum SST, and annual recruitment data (red), where PSST is the annual maximum SST for each year and site. The PSST for the forest cover models represents the 1982–2018 95th percentile annual maximum. Temperatures in the historical seedling experiment data are a subset from Rank et al.[30] and include data for PIPO and PSME. The RAP forest cover fraction and MODIS VCF canopy fraction were classified as forest using 10% and 20% thresholds. The EVT (Landfire) cover is categorical and includes conifer and mixed conifer–deciduous vegetation type classes.

https://doi.org/10.1038/s41561-024-01577-0

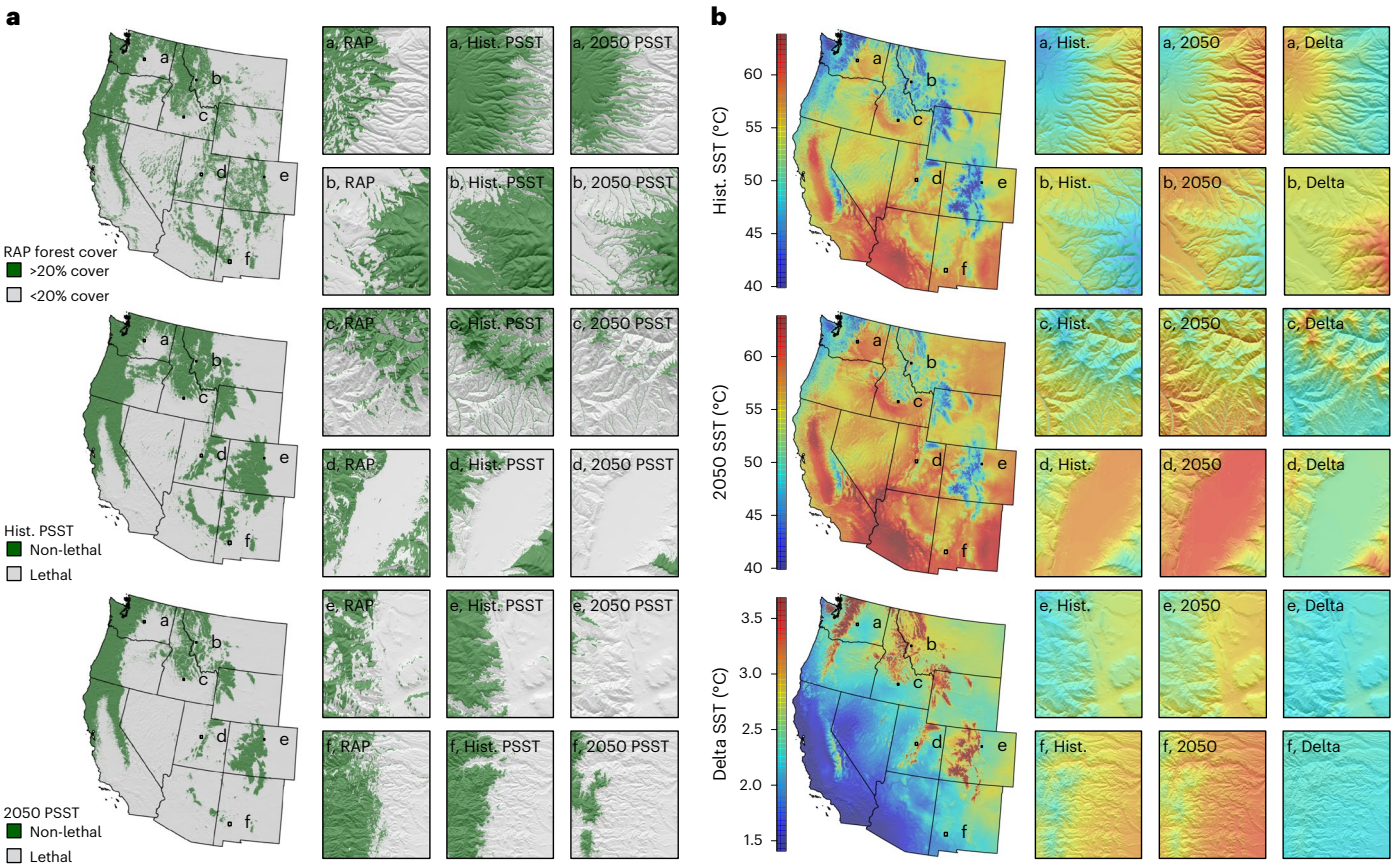

Fig. 2 | Soil surface temperatures contain low elevation forests. a, PSST and satellite-derived forest cover maps at low-elevation treeline positions a–f across the western United States: historical (Hist.) RAP forest cover data (20% threshold) (left column), the GWR model fit for the historical reference period (middle column) and the future (2050) projection (right column). **b**, Historical (1982–2018) and projected 2050 95th percentile annual maximum PSST for forest margins shown in **a**.

(Fig. 1). These experiments, summarized by Rank et al.[30] were conducted under well-watered conditions and thus isolate the effects of surface temperature on seedling mortality from hydraulic stress. Additionally, we find that logistic models of post-fire regeneration success that rely on space-for-time substitution[9] (N = 10,108, area under the receiver operating characteristics curve (AUC) of 0.74; Supplementary Table 1) and annually resolved recruitment data[31] (N = 1,840, AUC of 0.70; Supplementary Table 2) show sharp declines in the probability of post-fire conifer recruitment as PSST approach 50–60 °C. (Fig. 1). Finally, we compare simulated PSST and satellite-derived tree cover using logistic geographically weighted regression (GWR) (n = 210,000, GWR AUC of 0.91 and generalized linear model (GLM) AUC of 0.76–0.82). The forest cover response to PSST is congruent with both lab and field observations (Fig. 1), but demonstrates variation among canopy cover products and thresholds chosen to classify forest cover.

Overall, our findings support the hypothesis that conifer seedlings have a distinct thermal boundary defining the lower treeline and areal extent of western North American forests. Young seedlings are sensitive to elevated soil temperatures as first year germinants are poorly lignified and do not have well-developed bark or access to deeper soil moisture[17]. Heat conducted from the soil surface can cause irreversible damage to enzymes and proteins in the protoplasm and cell membranes, leading to stem damage and death[32]. Indeed, high SSTs have been recognized as a direct cause of seedling mortality since the early twentieth century[33]. High SSTs, in some instances, are a primary constraint on conifer regeneration. In other instances, they are probably a secondary indicator of dry soils. We cannot identify in all instances the specific mechanism of mortality—lethal surface temperatures or associated dry soils—as these variables are physically linked and highly correlated. Nonetheless, PSST provides a potentially important and useful indicator of the thermal constraints on western United States forests.

Mapping forest vulnerability to extreme surface temperatures

High-resolution maps of PSST, used as a predictor of forest cover, show agreement with low-elevation forest margins across the western United States (AUC of 0.91; Fig. 2). Comparing modelled and observed forest cover maps, we estimate that between 107,000 and 238,000 km^2 (dependent on forest cover product and threshold; Supplementary Table 3) of currently forested area has experienced PSST extremes that exceed threshold values as determined during our historical simulation period from 1982 to 2018 (Fig. 3). Projected estimates of PSST for 2050 exceeds historical values by more than 2 °C in most areas, with larger increases where soil moisture is projected to decline (Supplementary Figs. 1 and 2). These projections suggest that the area that can no longer support forest regeneration nearly doubles by 2050, with 333,000–450,000 km^2 of current forests experiencing lethal temperatures during the 2050 mean period (Fig. 2). To compare our results with recent research on low-elevation regeneration dynamics[9], we intersect our projected forest cover maps with range maps for PIPO and PSME. We find that more than 41,000 km^2 of PIPO and 23,000 km^2 of PSME forests have experienced threshold PSST events during the 1982–2018 period. We anticipate that, by 2050, the area that can support either species will decline by an additional 60,000 km^2 for both species (Supplementary Table 4).

https://doi.org/10.1038/s41561-024-01577-0

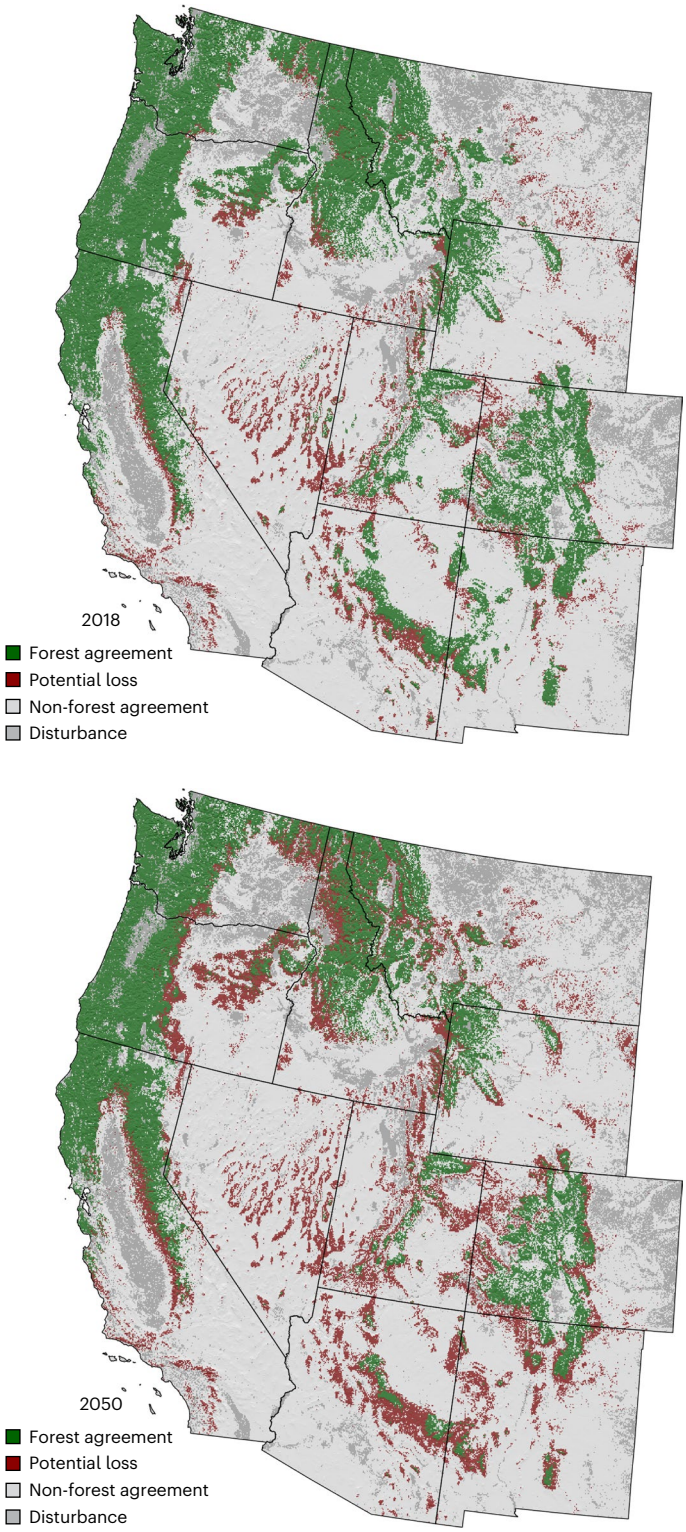

Fig. 3 | Projected change in modelled forest cover between 1982–2018 and 2050. The areas in red show currently forested areas where the PSST (°C) exceeds the limits for forest establishment. The areas in white indicate developed and agricultural areas according to Landfire EVT classes.

Soil temperature constraints on treeline dynamics have long been proposed for upper treelines[11,12]. Here, we extend this work to high SSTs and lower treelines. SST is a biophysical metric that integrates both the water and energy balance at a site and is governed primarily by net radiation and soil moisture. SST is related to land surface temperature (LST), which is a direct radiometric measure of the temperature at the Earth's surface[34,35]. SST and LST should be similar for bare soils, but deviate in vegetated areas and particularly forests, where canopies buffer temperature effects via latent heat exchange (Supplementary Figs. 3 and 4). LST can be observed via satellite allowing for analysis at multiple temporal and spatial scales[23,34]. However, direct measurements of LST for understanding the near-surface conditions that tree seedlings experience will be limited to post-disturbance observations in which overstories do not obscure direct inspection of these environments. In contrast, PSST is a simulated metric of temperature at the soil surface in the absence of an overstory and thus can be used for predicting potential for regeneration failure in undisturbed sites and in novel temporal and spatial domains. We demonstrate the consistency between LST and PSST (Supplementary methods and Supplementary Figs. 3 and 4) in non-forest areas to validate the performance of the ecohydrologic model we use (Ech2o[36]).

Simulating elements of the energy and water balance of post-fire environments is critical for understanding climate risks to regeneration in forests. PSST provides a direct mechanistic link to the multiple stressors currently affecting western United States forests including increased temperatures[5] and drought[17]. The gridded historical and future PSST maps developed here were designed to capture important physiographic details including cool areas of convergent terrain and cooler temperatures on shaded slopes; features of the landscape that managers use to maximize tree planting survival. These maps are available and intended to assist practitioners and land managers with adaptive management decisions.

Future climate projections portend drier and warmer summers[5] and enhanced wildfire activity[6]. The same factors that drive wildfires will challenge seedling survival following disturbance. As the planet warms, we expect the area that exceeds lethal temperature thresholds will increase, shifting low-elevation treeline upwards in elevation and decreasing the areal extent of forests. This process will not be gradual or linear but will unfold as an 'ecological ratchet'[14] catalysed by hot and dry years that drive fire activity and burned area, which will erode the extent of mature forests while simultaneously constraining the area where regeneration can occur[9,20]. As such, PSST can be used by scientists and managers alike to better define the biophysical boundary for feasible forest regeneration and to prioritize mitigation as the climate continues to change.

Online content

Any methods, additional references, Nature Portfolio reporting summaries, source data, extended data, supplementary information, acknowledgements, peer review information; details of author contributions and competing interests; and statements of data and code availability are available at https://doi.org/10.1038/s41561-024-01577-0.

References

1. Bonan, G. B. Forests and climate change: forcings, feedbacks, and the climate benefits of forests. *Science* **320**, 1444–1449 (2008).
2. Pan, Y. et al. A large and persistent carbon sink in the world's forests. *Science* **333**, 988–993 (2011).
3. Anderegg, W. R. L. et al. A climate risk analysis of Earth's forests in the 21st century. *Science* **377**, 1099–1103 (2022).
4. Allen, C. D. et al. A global overview of drought and heat-induced tree mortality reveals emerging climate change risks for forests. *For. Ecol. Manag.* **259**, 660–684 (2010).
5. IPCC *Climate Change 2021: The Physical Science Basis* (Cambridge Univ. Press, 2021).
6. Abatzoglou, J. T. & Williams, A. P. Impact of anthropogenic climate change on wildfire across western US forests. *Proc. Natl Acad. Sci. USA* **113**, 11770–11775 (2016).
7. Anderegg, W. R. L. et al. Tree mortality from drought, insects, and their interactions in a changing climate. *New Phytol.* **208**, 674–683 (2015).

8. Stevens-Rumann, C. S. et al. Evidence for declining forest resilience to wildfires under climate change. *Ecol. Lett.* **21**, 243–252 (2018).
9. Davis, K. T. et al. Reduced fire severity offers near-term buffer to climate-driven declines in conifer resilience across the western United States. *Proc. Natl Acad. Sci. USA* **120**, e2208120120 (2023).
10. Coop, J. D. et al. Wildfire-driven forest conversion in western North American landscapes. *BioScience* **70**, 659–673 (2020).
11. Körner, C. & Paulsen, J. A world-wide study of high altitude treeline temperatures. *J. Biogeogr.* **31**, 713–732 (2004).
12. Harsch, M. A., Hulme, P. E., McGlone, M. S. & Duncan, R. P. Are treelines advancing? A global meta-analysis of treeline response to climate warming. *Ecol. Lett.* **12**, 1040–1049 (2009).
13. Elsen, P. R. & Tingley, M. W. Global mountain topography and the fate of montane species under climate change. *Nat. Clim. Change* **5**, 772–776 (2015).
14. Jackson, S. T., Betancourt, J. L., Booth, R. K. & Gray, S. T. Ecology and the ratchet of events: climate variability, niche dimensions, and species distributions. *Proc. Natl Acad. Sci. USA* **106**, 19685–19692 (2009).
15. Pulliam, H. R. On the relationship between niche and distribution. *Ecol. Lett.* **3**, 349–361 (2000).
16. Tyree, M. T. Plant hydraulics: the ascent of water. *Nature* **423**, 923–923 (2003).
17. Kolb, P. F. & Robberecht, R. High temperature and drought stress effects on survival of *Pinus ponderosa* seedlings. *Tree Physiol.* **16**, 665–672 (1996).
18. League, K. & Veblen, T. Climatic variability and episodic *Pinus pondoras* establishment along the forest-grassland ecotones of Colorado. *For. Ecol. Manag.* **228**, 98–107 (2013).
19. Rother, M. & Veblen, T. Climate drives episodic conifer establishment after fire in dry ponderosa pine forests of the Colorado Front Range, USA. *Forests* **8**, 159 (2017).
20. Davis, K. T., Dobrowski, S. Z., Holden, Z. A., Higuera, P. E. & Abatzoglou, J. T. Microclimatic buffering in forests of the future: the role of local water balance. *Ecography* **42**, 1–11 (2019).
21. De Frenne, P. et al. Forest microclimates and climate change: importance, drivers and future research agenda. *Glob. Change Biol.* **27**, 2279–2297 (2021).
22. De Frenne, P. et al. Global buffering of temperatures under forest canopies. *Nat. Ecol. Evol.* **3**, 744–749 (2019).
23. Cooper, L. A., Ballantyne, A. P., Holden, Z. A. & Landguth, E. L. Disturbance impacts on land surface temperature and gross primary productivity in the western United States. *J. Geophys. Res. Biogeosci.* **122**, 930–946 (2017).
24. Daubenmire, R. & Slipp, A. W. Plant succession on Talus slopes in Northern Idaho as influenced by slope exposure. *Bull. Torrey Bot. Club* **70**, 473–480 (1943).
25. Baker, F. S. Effect of excessively high temperatures on coniferous reproduction. *J. For.* **27**, 949–975 (1929).
26. Choat, B. et al. Global convergence in the vulnerability of forests to drought. *Nature* **491**, 752–755 (2012).
27. Sapes, G. & Sala, A. Relative water content consistently predicts drought mortality risk in seedling populations with different morphology, physiology and times to death. *Plant Cell Environ.* **44**, 3322–3335 (2021).
28. Williams, A. P. et al. Temperature as a potent driver of regional forest drought stress and tree mortality. *Nat. Clim. Change* **3**, 292–297 (2013).
29. Simeone, C. et al. Coupled ecohydrology and plant hydraulics modeling predicts ponderosa pine seedling mortality and lower treeline in the US Northern Rocky Mountains. *New Phytol.* **221**, 1814–1830 (2019).
30. Rank, R., Maneta, M., Higuera, P., Holden, Z. & Dobrowski, S. Conifer seedling survival in response to high surface temperature events of varying intensity and duration. *Front. For. Glob. Change* https://doi.org/10.3389/ffgc.2021.731267 (2022).
31. Davis, K. T. et al. Wildfires and climate change push low-elevation forests across a critical climate threshold for tree regeneration. *Proc. Natl Acad. Sci. USA* **116**, 6193–6198 (2019).
32. Gates, D. M. *Biophysical Ecology* (Courier Corporation, 2012).
33. Hartley, C. Stem lesions caused by excessive heat. *J. Agric. Res.* 595–604 (1918).
34. Jin, M. & Dickinson, R. E. Land surface skin temperature climatology: benefitting from the strengths of satellite observations. *Environ. Res. Lett.* **5**, 044004 (2010).
35. Mildrexler, D. J., Zhao, M. & Running, S. W. A global comparison between station air temperatures and MODIS land surface temperatures reveals the cooling role of forests. *J. Geophys. Res. Biogeosci.* **116**, G03025 (2011).
36. Maneta, M. P. & Silverman, N. L. A spatially distributed model to simulate water, energy, and vegetation dynamics using information from regional climate models. *Earth Interact.* **17**, 1–44 (2013).

Methods

We used the spatially distributed ecohydrological model Ech2o[27,34] to develop a 30 m resolution model of 95th percentile PSST across the western United States for the 37 year period from 1982 to 2018. The surface energy balance component of Ech2o is a first-order local closure of radiative, conductive and turbulent energy fluxes in a soil layer of variable thickness. Soil heat capacity and conductivity is modulated by soil moisture. Equations for latent heat and sensible heat fluxes are based on similarity theory under neutral conditions. Latent heat fluxes from evaporation and from transpiration are solved separately using different heat conductance formulations. We simulated 3-hourly surface temperatures at a set of 61,200 randomly selected points, stratified by elevation, solar insolation and topographic wetness, with a 50% reduction in sampling density in areas with low-elevation relief. Spatial inputs for each point were created using the 30 m National Elevation Dataset and gridded soil maps[37] adjusted spatially based on calibration at existing soil moisture monitoring stations (Supplementary Figs. 5–9). We ran each simulation using a 210 m buffer around each focal point (7 × 7 grid cells of 30 m) to allow lateral water flow to sites in convergent terrain. Input temperature, humidity and radiation data were extracted from 250 m resolution daily weather grids[38] converted to hourly data following previously described methods[29]. Precipitation data were extracted from 4 km resolution daily PRISM grids[39] with hourly precipitation distributed uniformly for days with rain. We defined the vegetation for each point as a uniform bed of PIPO seedlings, with a canopy fraction of 10% and leaf area index of 1. We summarized hourly simulations of soil moisture and SST to daily minimum and maximum, respectively. We then calculated annual maximum and finally PSST, the 95th percentile annual maximum SST from 1982 to 2018.

Climate futures

We used data from the Sixth Coupled Model Intercomparison Project (CMIP6)[40] and a weather generator adapted from the R library rweathergen[41] to simulate daily time series of weather for the 2050 period using the Shared Socioeconomic Pathway 2-4.5 from the IPCC sixth assessment report. This scenario assumes that current emissions continue until 2050, with some reductions by 2100. Our selection of models was based primarily on data availability and considering guidance from recent downscaling work[42–44]. We searched the Pangeo repository (https://pangeo.io/ accessed March 2022) for monthly timestep general circulation model (GCM) simulation runs containing five or more replicate historical and SSP2-4.5 pairs and identified ten models meeting that criterion. We further screened these experiments, dropping the CANESM5, UKESM1 and IPSL-CSM6 models because they project increased warm season precipitation inconsistent with most other models (Supplementary Fig. 12). Additionally, we dropped the CSRM-MP6 in favour of the more advanced CSRM-ESM2 (ref. 43) and likewise chose the EC-Earth3 over the related EC-Earth3-veg model experiments[44]. The five models used to construct our ensemble mean are described in Supplementary Table 5. For each replicate within a model, we calculated monthly normals for the periods of 1984–2014 and 2035–2065. We then averaged over the replicates to get mean values for each GCM and again averaged the five GCM means to obtain a global mean. Delta values were calculated from the global means as the difference between future and historical for temperature and humidity, and as ratio of future/historical for precipitation, wind and solar radiation. Mean projected changes for our ensemble mean relative to the full set of available models are shown in Supplementary Fig. 12. Our five-model average is cool when compared with a larger ensemble, thus our PSST projections are probably somewhat conservative with respect to alternative future scenarios. Using a weather generator[41], we integrated projected monthly mean deltas with historical daily weather data extracted at each sample point to simulate 40 year daily weather inputs adjusted for the 2050 period. Using identical spatial and vegetation inputs as the historical runs, we simulated 3-hourly SSTs and then summarized the hourly data to obtain the PSST for the 2050 period.

Spatial mapping of PSST

We used GWR with a Gaussian kernel to interpolate the 95th percentile annual maximum surface temperature from 61,200 point simulations for the western United States using 30 m resolution elevation, solar radiation and topographic wetness as predictors[45]. This point-based simulation and mapping approach using a spatial buffer allows us to retain important model physics within a feasible computational expense. GWR models were evaluated across a range of adaptive bandwidths using leave-one-out cross-validation and root mean squared error (r.m.s.e.) as the objective function. We found that, while very small adaptive bandwidths produced the lowest error statistics, they gave implausible coefficient estimates (for example, positive elevation coefficients) with high spatial variability. Therefore, we subjectively selected bandwidths that gave competitive error stats and plausible coefficient estimates. The accuracy of the model was $R^2 = 0.77$ with an r.m.s.e. of 1.42 °C using the full dataset and $R^2 = 0.75$ with an r.m.s.e. of 1.42 °C using withheld observations. We used the final fitted model to project historical PSST at a spatial resolution of 30 m for the western United States. Sample points located in areas with high topographic convergence (>95th percentile TWI) were modelled separately and combined with the GWR maps (see Supplementary information for additional details). Projected 2050 PSSTs were first calculated as departures from historical (that is, deltas) at the sample point, then interpolated using GWR and added to the historical 30 m PSST map.

PSST and historical forest cover

We evaluated relationships between PSST and forest cover from three different 30 m resolution forest cover products: the Landfire Existing Vegetation Type (EVT), the MODIS vegetation continuous fields product (VCF)[46] and the Rangeland Analysis Platform (RAP)[47]. We combined annual forest cover fraction maps from RAP (1986–2018) and VCF (2002–2018) into annual maximum forest cover fraction maps to minimize effects from historical disturbances and then classified the composite maximum into binary (forest or non-forest) using 10% and 20% thresholds. We then used GWR (binomial family, logit link function) to model the relationship between PSST and forest occurrence. Models were evaluated across a range of bandwidths using leave-one-out cross-validation and using AUC as the objective function. Again, we selected bandwidths that were a compromise between fit statistics and reasonable coefficient estimates. The final 30 m resolution GWR prediction fit was then classified into a binary forest presence/absence map using an optimization function in the R library PresenceAbsence[48] to select a single threshold that maximized agreement with RAP forest cover. The optimal classification threshold ranged from 0.56 to 0.61 depending on whether overall accuracy, Kappa or AUC were used to optimize agreement. We used the median value of 0.58 to convert continuous GWR fit into a binary forest–no forest map.

Logistic survival model

We evaluated relationships between simulated SST and observations of heat-induced mortality summarized by Rank et al.[30]. The seedling survival data represent the proportion of trees surviving various duration and magnitude surface temperature exposures. From this larger dataset, we subset data to observations for PIPO and PSME from two historical studies[49,50] that shared a similar experimental design (20 seedlings per trial and similar heating apparatus) and had adequate replication (PIPO, 48 replicates and PSME, 103 replicates). These two species are widespread dominant conifers of low-elevation forests of the western United States. We fitted a binomial logistic regression using proportional survival as the response and measured SST as a predictor. The functional response of seedling survival to SST is thus represented as a probability of survival.

Post-fire conifer regeneration models

We analysed SST effects on post-fire conifer recruitment with data from two recent western United States studies. First, we extracted the 95th percentile annual maximum surface temperature from the 30 m resolution interpolated PSST model at 10,108 post-fire plots used by Davis et al.[9]. We refer to these as 'spatial' recruitment data, as the analysis uses a space-for-time substitution and the precise year (and annual conditions) of recruitment is unknown. We then re-fitted the all-species linear mixed effects model described in ref. 9 but with PSST included as a fixed predictor while excluding heat load index. We evaluated a set of candidate LME models that included interactions described in ref. 9 as well as interaction terms suggested during exploratory analysis using boosted regression trees. A final mixed effects regression model included fire as a random effects and PSST, 30 year mean annual climatic water balance deficit, distance to live tree, fire severity and surrounding tree cover as fixed effects (AUC of 0.73; Supplementary Table 1).

Last, we re-analysed annual post-fire recruitment data for PIPO and PSME collected across the western United States[31]. This dataset includes 89 sites from 32 unique fires but resolves the annual year of recruitment, such that estimated climatic conditions in each year can be correlated directly with seedling establishment. Here, we simulated SST at each plot from 1982 to 2015 and then summarized the 3-hourly data to return the maximum annual SST for each plot and year. We analysed SST effects on annual recruitment using LME models with random intercept terms for fire and plots within fires to account for repeated annual measurements at each sample site. A final mixed effects regression model included annual SST, distance to seed source and time since fire (AUC of 0.70; Supplementary Table 2).

Data availability

All data that support the findings of this study are openly available at the references provided. New and derived datasets, including seedling experiments and 30 m gridded surface temperature predictions, are available via Figshare at https://doi.org/10.6084/m9.figshare.26950843 (ref. 51).

Code availability

The data and code that support the findings of this study are available via Figshare at https://doi.org/10.6084/m9.figshare.26950843 (ref. 51).

References

37. Ramcharan, A. et al. Soil property and class maps of the conterminous United States at 100-meter spatial resolution. *Soil Sci. Soc. Am. J.* **82**, 186–201 (2018).
38. Holden, Z. A. et al. Decreasing fire season precipitation increased recent western US forest wildfire activity. *Proc. Natl Acad. Sci. USA* **115**, E8349–E8357 (2018).
39. Daly, C. et al. Physiographically sensitive mapping of climatological temperature and precipitation across the conterminous United States. *Int. J. Climatol.* **28**, 2031–2064 (2008).
40. Eyring, V. et al. Overview of the Coupled Model Intercomparison Project Phase 6 (CMIP6) experimental design and organization. *Geosci. Model Dev.* **9**, 1937–1958 (2016).
41. Steinschneider, S. & Brown, C. A semiparametric multivariate, multisite weather generator with low-frequency variability for use in climate risk assessments. *Water Resour. Res.* **49**, 7205–7220 (2013).
42. Mahony, C. R., Wang, T., Hamann, A. & Cannon, A. J. A global climate model ensemble for downscaled monthly climate normals over North America. *Int. J. Climatol.* **43**, 5871–5891 (2022).
43. Séférian, R. et al. Evaluation of CNRM Earth System Model, CNRM-ESM2-1: role of earth system processes in present-day and future climate. *J. Adv. Model. Earth Syst.* **11**, 4182–4227 (2019).
44. Döscher, R. et al. The EC-Earth3 Earth system model for the Coupled Model Intercomparison Project 6. *Geosci. Model Dev.* **15**, 2973–3020 (2022).
45. Hoylman, Z. A 30 m topographic wetness index dataset for the continental United States. *Zenodo* https://doi.org/10.5281/zenodo.4460353 (2021).
46. Carroll, M. et al. in *Land Remote Sensing and Global Environmental Change: NASA's Earth Observing System and the Science of ASTER and MODIS* (eds Ramachandran, B., Justice, C. O. & Abrams, M. J.) 725–745 (Springer, 2011).
47. Allred, B. W. et al. Improving Landsat predictions of rangeland fractional cover with multitask learning and uncertainty. *Methods Ecol. Evol.* **12**, 841–849 (2021).
48. Freeman, E. A. & Moisen, G. PresenceAbsence: an R package for presence absence analysis. *J. Stat. Soft.* **23**, 1–31 (2008).
49. Seidel, K. Tolerance of seedlings of ponderosa pine. Douglas-fir, grand fir, and Engelmann spruce for high temperatures. *Northwest Sci.* **60**, (1986).
50. Silen, R. R. *Lethal Surface Temperatures and Their Interpretation for Douglas-Fir*. Corvallis, OR: Oregon State University. 170p. PhD thesis (1960).
51. Holden, Z. A. et al. Data repository: Low-elevation forest extent in the western United States constrained by soil surface temperatures. *Figshare* https://doi.org/10.6084/m9.figshare.26950843 (2024).

Acknowledgements

Computational resources from the University of Montana's Computational Ecology Lab, NASA Pleiades HPC cluster and the Griz Shared Computing Cluster contributed to this research (NSF award numbers 2018112 and 1925267). We thank the editors and three anonymous reviewers for comments and feedback that improved the final manuscript. We thank the Montana Climate Office for access to soil moisture observations. This work was supported with funding from the National Aeronautical and Space Administration (grant 80NSSC19K00181) and the USDA NIFA (grant 2022-67019-36438).

Author contributions

Z.A.H., S.Z.D. and M.M. designed the research. Z.A.H., D.L., A.S., A.W. and S.Z.D. performed the research and data analysis. S.Z.D, Z.A.H., Z.H., M.M. and A.S. wrote the manuscript. All authors contributed to revising the final manuscript.

Competing interests

The authors declare no competing interests.

Additional information

Supplementary information The online version contains supplementary material available at https://doi.org/10.1038/s41561-024-01577-0.

Correspondence and requests for materials should be addressed to Zachary A. Holden.

Peer review information *Nature Geoscience* thanks Courtney Collins, Florian Zellweger and the other, anonymous, reviewer(s) for their contribution to the peer review of this work. Primary Handling Editor: Xujia Jiang, in collaboration with the *Nature Geoscience* team.